Chiang Mai J. Sci. 2020; 47(3) : 362-377
http://epg.science.cmu.ac.th/ejournal/
Contributed Paper

Effect of Actinomycin D Isolated From the Cultured Broth of Marine *Streptomyces* spp. on Cell Division Protein FtsZ

Phennapa Charoenwiwattanakij [a], Jaturong Pratuangdejkul [b], Sumet chongruchiroj [b], Khanit Suwanborirux [c], Chitti Thawai [d], Jiraporn Chingunpitak [e] and Veena Satitpatipan*[a]

[a] Department of Pharmacognosy, Faculty of Pharmacy, Mahidol University, Bangkok, Thailand.
[b] Department of Microbiology, Faculty of Pharmacy, Mahidol University, Bangkok, Thailand.
[c] Department of Pharmacognosy and Pharmaceutical Botany, Faculty of Pharmaceutical Sciences, Chulalongkorn University, Bangkok, Thailand.
[d] Department of Biology, Faculty of Sciences, King Mongkut's Institute of Technology Ladkrabang, Bangkok, Thailand.
[e] School of Pharmacy, Walailak University, Nakhon Si Thammarat, Thailand.

*Author for correspondence; e-mail: veena.nuk@mahidol.ac.th

Received: 18 September 2019
Revised: 31 January 2020
Accepted: 5 February 2020

ABSTRACT

In the course of our investigation on antibacterial substances with FtsZ inhibitory effect, actinomycin D was isolated from the ethyl acetate extract of *Streptomyces* sp. LT3-17. The compound showed antibacterial activities. The MIC values of actinomycin D against *Staphylococcus aureus* ATCC 25923, Methicillin-resistant *Staphylococcus aureus* DMST 20654, *Bacillus subtilis* ATCC 6633, *Escherichia coli* ATCC 25922, and *Pseudomonas aeruginosa* ATCC 27853 were 3.13, 0.39, 0.10, 300.00, and 500.00 μg/mL, respectively. The morphology study of *E. coli* JW0093 treated with the compound showed inhibitory effect on cell elongation. The inhibition of FtsZ activity by actinomycin D was shown as the inhibition of GTPase activity with IC_{50} value, 20.06 μM. The polymerization of *E. coli* FtsZ protein (*Ec*FtsZ) treated with 0.01 μM actinomycin D showed the degree of polymerization ratio was less than 1.0 indicating the inhibitory potential of actinomycin D on FtsZ polymerization. *In silico* study was performed to predict binding mode of actinomycin D into nucleotide binding pocket of the homology model of *Ec*FtsZ protein. From the results of these experiments, the isolation and elucidation methods of actinomycin D as well as its novel mechanism as FtsZ inhibitors have been discovered.

Keywords: actinomycin D, antibacterial agent, FtsZ, marine, *Streptomyces*

1. INTRODUCTION

Bacterial resistance to antibiotics is known as one of the major global health problems. This causes by high mutation rate of bacteria since they can effectively adapt to the change in environment as well as inappropriate uses of antibacterial drugs. In order to solve this problem, various antibacterial agents have been isolated and developed along with finding of new specific targets. Cell division has been considered as one of promising targets for antibacterial drug discovery [1, 2].

Cell division is an attractive antibacterial target. In this step, there are several essential proteins

which will cause major disruption to prokaryotic cell if they work abnormally. Due to several features, currently cell division is considered as a novel antibacterial target. Firstly, components involved in cell division process are necessary to cytokinesis which results in bacterial growth. The next supporting reason is conservation of proteins in this process which mostly restrictedly distribute among prokaryotes [3]. Among these proteins, Filamenting temperature sensitive mutant Z (FtsZ) is a vital protein in bacterial cell division. This 40-KDa protein is a major protein responsible for cytokinesis in bacteria. FtsZ protein is considered as tubulin homolog in eukaryotes. However, it shares only 20 % similarity between their amino acid sequences. Furthermore, FtsZ is conserved in prokaryotes in genetic level and its existence is preserved only in this kingdom [4, 5]. It also shows a high degree of similarity among bacterial species and evolutionarily distant from tubulin. This discovery kindles the hope of new attractive target for antibacterial agents, which is specific to bacterial cells [6, 7]. Since FtsZ protein is a homolog of tubulin, it also possesses same activity as GTPase. In biological pathway, GTPase enzymatic activity is very important in transport, signal transduction, protein biosynthesis and especially cell differentiation. By using GTP as energy source, FtsZ monomer hydrolyzes this substance into GDP and free phosphate ion for polymerization of FtsZ monomers to form Z ring [5].

In our study, sources of antibacterial agents as FtsZ inhibitors were scrutinized. Many compounds from terrestrial plants and chemical synthesis were found to process the ability to inhibit FtsZ protein. However, only few compounds from marine sources were found to contain this activity [8-10]. In studies of marine natural products, actinomycetes are well known for their potential to produce antibiotics. Actinomycetes are an important source for natural products with biological activities. As approximately 22,500 bioactive secondary metabolites are produced by microorganisms and more than 10,000 of these compounds (45% of microbial active secondary metabolites) are produced by actinomycetes [11]. Among this, majority of active compounds are produced by *Streptomyces* species which cover 70-80 % of total compounds. From this perspective, marine *Streptomyces* are currently viewed as an outstanding source of bioactive natural compounds due to compounds with wide range of structures and various potent biological activities [12].

2. MATERIALS AND METHODS

2.1 Test Microorganisms

2.1.1 Sample collection, isolation of actinomycetes and test microorganisms

Streptomyces strain LT3-17 was isolated from marine sediments collected from Lanta islands, Krabi province, Thailand, using the modified isolation method described by Thawai *et al.* [13]. Briefly, the marine sediment sample was air-dried at room temperature for 3 days. The dried sediment sample was then grounded and heated at 100°C for 1 h. The treated soil was serially diluted to the 10^{-3} concentration in 0.01% sterile sodium lauryl sulfate in distilled water and spread on starch-casein nitrate agar (10 g soluble starch, 1 g sodium caseinate (Difco, USA), 0.5 g KH_2PO_4, 0.5 g $MgSO_4$ and 18 g agar in 1 L of sea water, pH 8.3) supplemented with 25 mg L^{-1} nalidixic acid, 50 mg L^{-1} cycloheximide and 50 mg L^{-1} nystatin for 21 days at 30 °C. The actinomycete isolates were purified on ISP2 medium modified with seawater instead of distilled water.

The test microorganisms, *Staphylococcus aureus* ATCC 25923, *Bacillus subtilis* ATCC 6633, Methicillin-resistant *Staphylococcus aureus* DMST 20654, *Pseudomonas aeruginosa* ATCC 27853 and *Escherichia coli* ATCC 25922, were purchased from Culture Collection for Medical Microorganism, Department of Medical Sciences, Ministry of Public Health, Thailand. *E. coli* JW0093 was obtained from National BioResource Project Japan (NBRP)-*E. coli*/*B. subtilis*, Japan. The GTP and GTPase assay kit were purchased from Innova

Biosciences (UK). Purified *E. coli* FtsZ (*Ec*FtsZ) protein was purchased from Cytoskeleton Inc (USA). Isopropyl β-d-thiogalactopyranoside (IPTG) and ethylenediaminetetraacetic acid (EDTA) were purchased from Amresco (USA). Tetracycline was purchased from T.P. Drug Laboratories. The components of Luria broth (LB); sodium chloride, tryptone, and yeast extract were purchased from Biobasic Inc (Canada). Muller-Hilton agar and Muller-Hilton broth (MHB) were purchased from Difco (USA). Buffer components: Tris hydrochloride (Tris HCl) was purchased from Usb corporation; Magnesium acetate ($MgAcO_2$) and sodium chloride (NaCl) were purchased from Sigma Aldrich.

2.1.2 Identification of actinomycete strain LT3-17

2.1.2.1 16S rRNA analysis

The actinomycete strain, LT3-17, was taxonomically characterised using polyphasic approaches, including morphology of hyphae and spores, chemotaxonomic and 16S rRNA gene sequence analysis. To observe the morphological characteristics, the strain was cultured on ISP2 sea water agar for 14 days at 30°C and was then observed using light microscopy and scanning electron microscopy (model JSM-5410 LV; JEOL). Samples for scanning electron microscopy were prepared as described previously by Thawai *et al.* [14] and Thawai [15]. The colors of mycelium and spore were determined using the National Bureau of Standards/Inter Society Color Council (NBS/IBCC) color system [16]. To analyse the genotypic property, the actinomycete strain was grown on ISP2 broth, and cells were harvested for genomic DNA extraction according to the previously described method [17]. Amplification of the nearly complete 16S rRNA gene was performed using the universal primers 20F (5'-GAGTTTGATCCTGGCTCAG-3', positions 9–27) and 1541R (5'-GTTACCTTGTTACGACTT-3') [18]. The temperature profile was as follows: initial denaturation at 94°C for 3 minutes; 40 cycles of 94°C for 30 seconds, 56°C for 30 seconds, and 72°C for 90 seconds; and final extension at 72°C for 5 minutes. Sequencing of the PCR product was carried out using the 27F, 1492R, 350F (5'-TACGGGAGGCAGCAG-3'), 780F (5'-GATTAGATACCCTGGTAG-3'), 1100F (5'-GCAACGAGCGCAACCC-3'), 350R (5'-CTGCTGCCTCCCGTAG-3') and 780R (5'-CTACCAGGGTATCTAATCC-3') primers [19]. Subsequently, the pairwise alignment analysis of the 16S rRNA gene sequence of the actinomycete strain was performed on the EzTaxon server [20]. The CLUSTAL W programme, version 1.81 [21], was used for the multiple alignment analysis of the nearly complete 16S rRNA gene sequence of the strain and sequences of the members of the genus *Streptomyces*. Phylogenetic trees were reconstructed using neighbour-joining (NJ tree) [22] method in the programme MEGA version 6.0 [23]. The confidence levels of clusters were determined based on the bootstrap analysis with 1,000 resamplings [24].

2.1.2.2 DNA-DNA hybridization

DNA-DNA relatedness between strain LT3-17 and its phylogenetically closest relative, *Streptomyces parvulus* NBRC 13193^T, was studied in microdilution-well plates [25].

2.1.3 Isolation of actinomycin D

Streptomyces strain LT3-17 was cultured in ISP2 broth (pH 7.3) for 14 days. Then, the crude extract was obtained from partitioning the filtered media with ethyl acetate. Then, ethyl acetate crude extract was separated for pure active compounds. In order to find active compounds, both crude extracts and their separated fractions were investigated for antibacterial activities. The fractions with the activities were further separated by chromatographic techniques.

Ethyl acetate crude extract of LT3-17 was chromatographed using sephadex LH-20 as a stationary phase and CH_2Cl_2: EtOAc (8:2) as a mobile phase. Based on the results in bioautography and

morphological experiments, active fraction which possibly contained FtsZ inhibitor was selected for further separation by a silica gel column and eluted with gradients of mixtures; CH_2Cl_2-EtOAc (100:0 to 0:100) and EtOAc-MeOH (100:0 to 0:100). As the result, actinomycin D was obtained and the structure was confirmed by NMR, MS, UV and IR.

2.2 Investigation of Antibacterial Activity and FtsZ Inhibitory Activity

2.2.1 Minimum inhibitory concentration (MIC) and minimum bactericidal concentration (MBC)

Minimum inhibitory concentration (MIC) and minimum bactericidal concentration (MBC) against *S. aureus* ATCC 25923, *B. subtilis* ATCC 6633, MRSA DMST 20654, *P. aeruginosa* ATCC 27853 and *E. coli* ATCC 25922 were determined in accordance with the guidelines of Clinical and Laboratory Standards Institute. Bacterial susceptibility was tested using broth microdilution technique. MIC was defined as the lowest concentration of actinomycin D that caused no growth when detected turbidity with spectrophotometry at 600 nm (OD_{600}). Culture of bacteria with samples at concentrations of MIC and higher values were streaked on Mueller Hinton agar to determine the MBC values [26].

2.2.2 Observation of actinomycin D on morphology analysis of *E. coli* JW0093

E. coli JW0093 was cultured in Luria broth (LB) with 100μM IPTG and 25 μM tetracycline, overnight and diluted to concentration equal to OD_{600} = 0.1. Then, actinomycin D at final concentration of 0.1 μM in 1% DMSO were added to the cultures. The cultures were taken after 3 hours of incubation for Gram's stain and observed with 100x bright-field light microscope. The average cell-lengths were measured by CellSense Dimension program and then recorded by an Olympus digital camera [27].

2.2.3 Effect of actinomycin D on GTPase activity of *Ec*FtsZ

GTPase activity of purified *Ec*FtsZ protein was assayed in both the absence and presence of compounds at various concentrations (0-1,000 μM). The reactions were performed according to the protocol of the GTPase assay kit from Innova Biosciences, Inc. Briefly, purified *Ec*FtsZ protein (4 μM) was mixed with actinomycin D (0-1,000 μM) in the ratio of 1:1 and placed at 37°C for 30 minutes. Then 0.5 mM GTP in Tris buffer pH 6.5 was added. The reaction was incubated at 37°C for another 30 minutes. Finally, the detecting agent consisting of a malachite green solution was mixed to detect the phosphate amounts released at the end of the reaction. The result was read under a wavelength of 635 nm using a Tecan's Infinite® M200 Nanoquant UV microplate spectrometer. The results were reported as relationship between percentages of FtsZ activity and concentrations of actinomycin D for the determination of IC_{50} of FtsZ activity [27].

2.2.4 Polymerization assay

In order to form Z-ring, FtsZ molecule must be polymerized using GTP as the substrate. The polymerization leads to differences in the size of the polymer. In this study, a dynamic light scattering technique was adapted to detect the polymerization of *Ec*FtsZ. *Ec*FtsZ protein (4 μM) was mixed with actinomycin D in a Tris buffer consisting of 20 mM Tris, 40 mM NaCl, 4 mM $MgAcO_2$, 0.5 mM EDTA (pH 7.5, respectively. Then, 0.5 mM GTP was added and incubated at 37°C for 20 minutes. Derived count rate (DCR) at 0-30 minutes was detected by Zetasizer Nano-ZS [27]. Then data was subtracted from the control data (experiment without *Ec*FtsZ) and calculated for the ratio of polymerization as follows:

$$\text{Polymerization ratio} = \frac{(DCR_{experiment} - DCR_{control})}{(DCR_{experiment,\ 0\ min} - DCR_{control,\ 0\ min})}$$

2.3 *In silico* Studies of Actinomycin D at Nucleotide Binding Site of *Ec*FtsZ

The structure of actinomycin D was drawn using ChemBioDraw Ultra 11.0. All molecular modelling tools, analyses and visualization used in this study were performed using Discovery Studio 3.5 running on a work station with Intel Corei7 2.66 GHz with 6 GB of RAM with both Windows and Linux operating systems [27].

The binding of actinomycin D to *Ec*FtsZ were investigated by docking these compounds into the nucleotide binding site of the *Ec*FtsZ model using a flexible docking protocol in DS 3.5. Flexibility was allowed in the following residues: Val-130, Thr132, Phe-135, Phe-182, Asn-186, Leu-189, Lys-190 and Val-193. The docking protocol parameters were changed from the default values as follows: a 15.8 Å of docking sphere was defined, the maximum number of protein conformations was limited to 100 conformations of protein for flexible docking. BEST algorithm was applied to generate ligand conformations. Maximum conformation was set to 255 conformations in order to ensure the best coverage of the compound's conformational space. Number of hotspots used to define number of polar or apolar receptor and conformer matching was set to 200. Number of top docking poses, defined as top hits, was set to 100. The docking refinement was performed using simulated annealing refinement cycle consisting of 2,000 heating steps with the target temperature of 700K and 5,000 cooling steps with target temperature of 300K [28].

Determination for the best possible binding complex of each domain was performed. Ten best-binding complexes were selected by considering results from CDOCKER energy and CDOCKER INTERACTION energy. Then, energy minimization was performed on each of these FtsZ-inhibitor binding complexes. Binding energy was calculated on minimized complexes. The complex with the lowest binding energy was considered as the best FtsZ-inhibitor binding complex. Then the complex structure stability was optimized by molecular dynamics (MD) simulation using NAMD software [29] with CHARMm force field [30]. The complex was solvated in the TIP3P water box. The charge of the system was neutralized with an appropriate number of Na^+ and Cl^- counterions. Initially, the system was minimized by conjugate gradient method following by heating and equilibration using NPT ensemble at 310 K and 1 atm which was controlled by the Nosé-Hoover Langevin piston method [31]. Periodic boundary conditions (PBC) were set to avoid truncation effects. A Particle Mesh Ewald (PME) method [32] was used for calculation of long-range electrostatic forces. The full system was run for 10 ns with 2 fs time steps and SHAKE algorithm. The trajectories were saved every 2 ps for analysis. The stability of structure was evaluated using root mean square deviation (RMSD). Finally, the complex was further studied for interaction energy by calculating amino acid residues within 4Å around a docked inhibitor. The interacting residues of *Ec*FtsZ with an inhibitor were illustrated by ligand binding pattern; such as, hydrogen bond donors and acceptors, polar and nonpolar contacts implicated in protein main-chain as well as side-chain atoms. Discovery Studio Visualizer program (v17.2) was used to generate two-dimensional interaction of FtsZ-inhibitor complex and surrounding binding site residues. The complex pose with the lowest binding energy was chosen to study the binding mode interaction of actinomycin D in the nucleotide binding site of *Ec*FtsZ [28].

3. Results and Discussions

3.1 Identification of Strain LT3-17

The morphological, chemotypic and genotypic properties of strain LT3-17 are consistent with its classification in the genus *Streptomyces*. The strain produced well-developed and branched substrate hyphae on International *Streptomyces* Project 2 (ISP 2) medium. LT3-17 formed brownish yellow substrate mycelium and light grey aerial spore mass. The long spiral chains of smooth surfaced spores were observed on strain LT3-17 (Figure 1). This

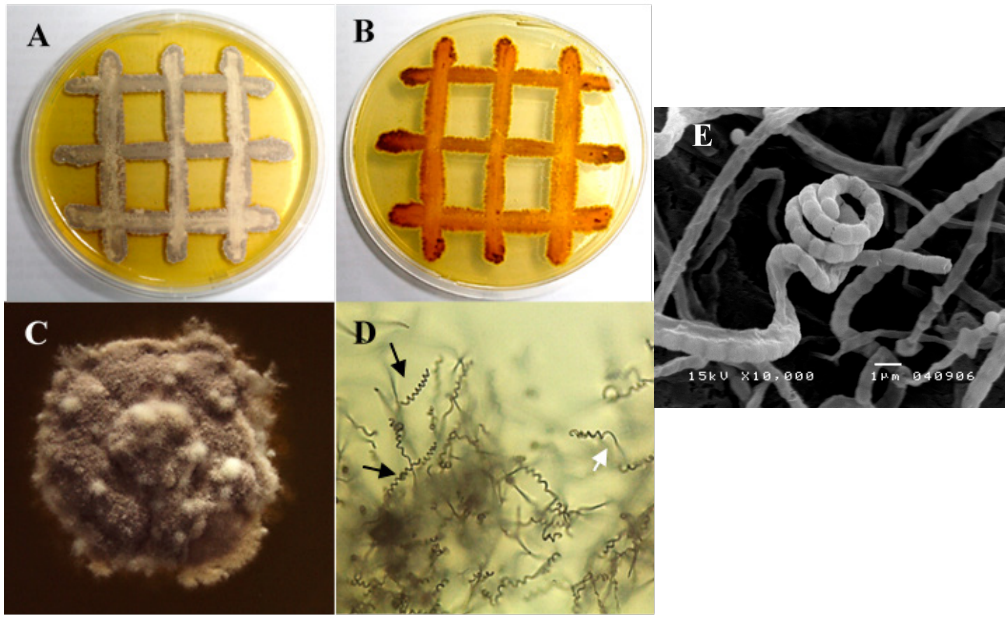

Figure 1. The colonial appearance of strain LT3-17 cultured on ISP 2 sea water agar. A-B, the upper and reverse side of colony; C, color and morphology of LT3-17 colony under stereomicroscope; D, aerial mycelium (white arrow) and spore (black arrows) observed under light microscope with long working distance lens (40X); E, SEM micrograph of strain LT3-17.

strain produced pale brownish diffusible pigments in medium. Cell wall of strain LT3-17 contained *LL*-diaminopimelic acid. This confirmed the affiliation of the strain to the genus *Streptomyces*. To confirm the taxonomic position of this strain, the 16S rRNA gene sequencing was performed. The result revealed that strain LT3-17 was most closely associated and formed the closest clade with *Streptomyces parvulus* NBRC 13193^{T} in the neighbour joining tree (99% bootstrap value) (Figure 2). The strain exhibited 100% 16S rRNA gene sequence similarity value with the reference strain mentioned above. Moreover, DNA-DNA relatedness between strain LT3-17 and *Streptomyces parvulus* NBRC 13193^{T}, the closest relative, was 81.3 ± 0.4%. These values were well above the 70% cut-off level that was used for assigning two bacterial strains to the same species [33]. Hence, strain LT3-17 was identified as *Streptomyces parvulus*.

3.2 Structure Determination of Actinomycin D

Actinomycin D (Figure 3) was isolated from *Streptomyces* LT3-17 as an orange crystalline in isolation yield of 20.65%. Its molecular weight was obtained from ESI-HR mass spectrum showing a pseudomolecular ion peak $[M+Na]^{+}$ at m/z 1,277.6179 implying a molecular formula of $C_{62}H_{86}N_{12}O_{16}$ (Calculated for $C_{62}H_{86}N_{12}O_{16}Na^{+}$; 1,277.6183). The UV spectrum in methanol displayed λ_{max} (log ε) at 243 (4.86) and 446 (4.46) nm. The IR spectrum (KBR disc) displayed the absorption with υ_{max} at 3,385, 3,264 cm^{-1} referring to an amide group. Moreover, there were several signals with υ_{max} at 1,682, 1,670, and 1,646 cm^{-1} which confirmed the presence of an amide carbonyls. υ_{max} at 1,747 cm^{-1} was also detected indicating the presence of ester carbonyls. The 500 MHz ^{1}H-NMR spectral data (in DMSO-d_6) of actinomycin D presented eighty-four proton signals separated into thirteen methyl proton signals

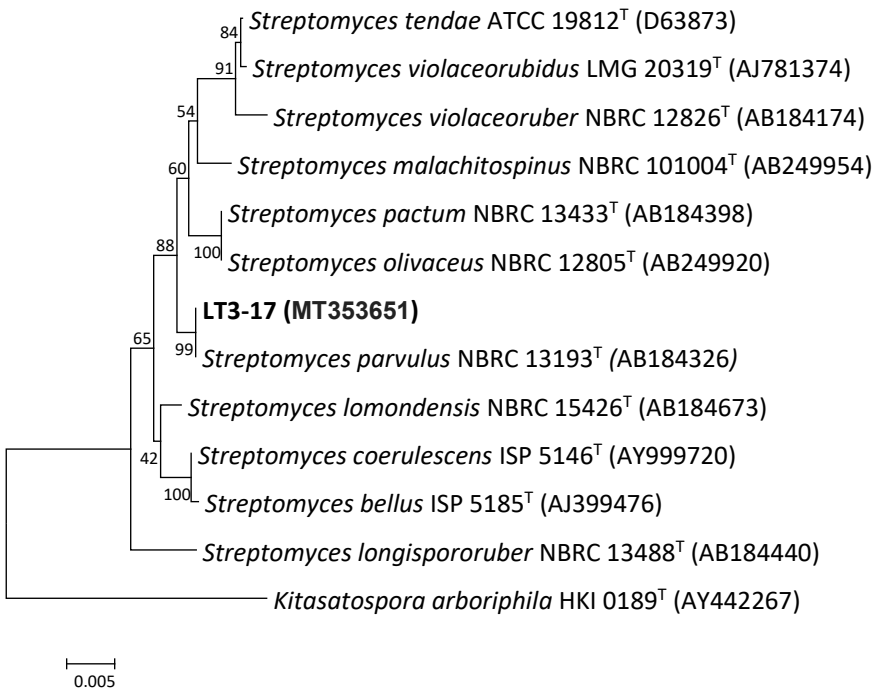

Figure 2. Phylogenetic tree based on the nearly complete 16S rRNA gene sequences (1,412 nt) of strain LT3-17. Numbers on branches represent the bootstrap values as the percentage of 1000 replicates. Only values > 50% are shown. Bar, 0.005 substitutions per nucleotide position.

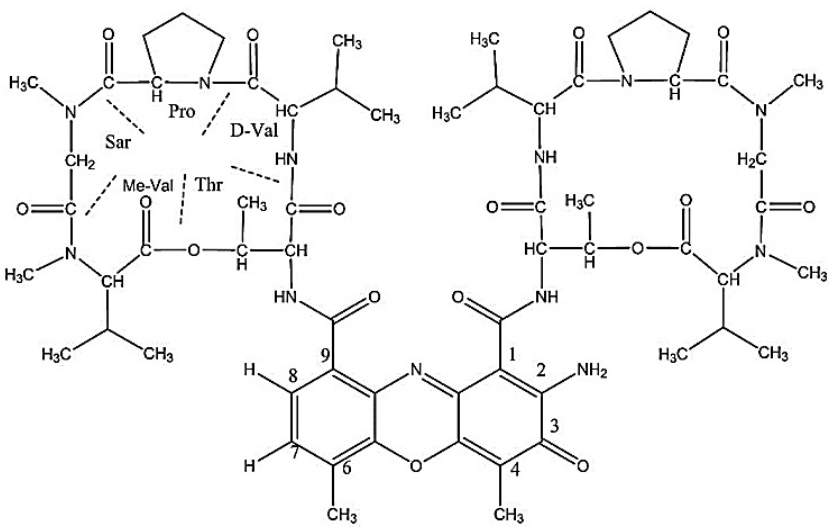

Figure 3. Structure of actinomycin D.

[δ 0.73 (6H), 0.87, 0.90, 0.94, 0.96, 1.10, 1.12, 1.24 (6H), 2.23, 2.54, 2.87, 2.90, and 2.92 ppm], ten signals of methylene proton [δ 1.83 (4H), 2.06, 2.28, 2.65 (4H), 3.59, 3.61, 3.71, 3.82, 4.72, and 4.80 ppm], ten methine proton signals [δ 2.09, 2.65 (4H), 3.54, 4.51, 4.62, 5.23, 5.93, 6.00, 7.36, and 7.61 ppm] and four amide proton signals [δ 7.17, 7.73, 8.02, and 8.19 ppm]. The 125 MHz ^{13}C-NMR spectral data (in DMSO-d_6) exhibited sixty-two carbon signals which supported the molecular formula $C_{62}H_{86}N_{12}O_{16}$. The spectral data of the compound was confirmed by comparing to previous reports and the result suggested that the obtained compound was actinomycin D [34, 35].

3.3 Antibacterial Activity and FtsZ Inhibitory Activities of Actinomycin D

3.3.1 Minimum inhibitory concentration (MIC) and Minimum bactericidal concentration (MBC)

Minimum inhibitory concentration (MIC) and minimum bactericidal concentration (MBC) of actinomycin D against *S. aureus* ATCC 25923, *B. subtilis* ATCC 6633, MRSA DMST 20654, *P. aeruginosa* ATCC 27853, *E. coli* ATCC 25922, and *E. coli* JW0093 were shown in Table 1.

The starting concentration of actinomycin D for MIC investigation was started at 500.00 μg/mL. Actinomycin D inhibited the growth of *S. aureus* ATCC 25923, *B. subtilis* ATCC 6633, and MRSA DMST 20654 with MIC values of 3.13, 0.30, 0.10, and 0.02 μg/mL, respectively. While, the activities against gram negative bacteria, *E. coli* ATCC 25922, *E. coli* JW0093, and *P. aeruginosa* ATCC 27853 were shown with MIC values of 300.00, 50.00, and 500.00 μg/mL, respectively. Then the experiments were further performed to determine MBC values of actinomycin D on sensitive strains. The results showed that actinomycin D had MBC values only against *S. aureus* ATCC 25923, *B. subtilis* ATCC 6633, and MRSA DMST 20654 at 12.50, 1.56, and 0.39 μg/mL, respectively.

3.3.2 Effect of actinomycin D on bacterial cell division

In normal binary fission process of bacteria, a single cell is generally separated into 2 daughter cells with equal shapes and sizes. Because the cytokinesis of bacterial cells was controlled by FtsZ, thus by adding FtsZ inhibitor; interference with process of the normal cell division was expected and would result as cell elongation and filamentous formation.

After 3 hours of incubation, the typical cell morphology of *E. coli* JW0093 was visualized under a microscope in a control of 1% DMSO (Figure 4). Treatment with 0.1 mg/mL of actinomycin D changed the morphology of the *E. coli* cells (Figure 4). Atypical characteristics for the inhibition of cell divisions with a nearly increased cell length was observed. Actinomycin D treated cells had an average length of 23.58±0.67

Table 1. The results of MIC and MBC values of actinomycin D.

Microorganisms	MIC (μg/mL) *	MBC (μg/mL) *
S. aureus ATCC 25923	3.13	12.50
MRSA DMST 20654	0.39	1.56
B. subtilis ATCC 6633	0.10	0.39
E. coli ATCC 25922	300.00	> 500.00
E. coli JW0093	50.00	> 500.00
P. aeruginosa ATCC 27853	500.00	> 500.00

ND; Experiment was not determined.
* starting concentration was 500.00 μg/mL.

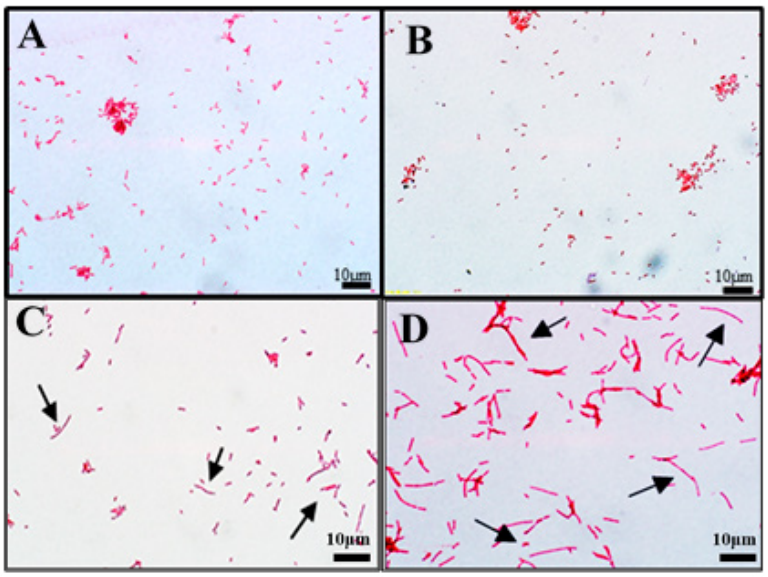

Figure 4. Light microscope images with average cell lengths of *E. coli* JW0093. A, growth control (untreated cells); B, negative control (1% DMSO treated cells); C, positive control (0.1 mg/mL berberine treated cells); D, Cells treated with 0.1 mg/mL of actinomycin D. A 10-µm bar is shown at the right-bottom corner of the pictures. The arrows pointed to the elongated cells.

as compared to the average length of 1.99±0.06, 2.08±0.11, and 5.90±0.85 µm for the bacterial growth control (untreated), negative control (1% DMSO) and positive control (0.1 mg/mL berberine) treated *E. coli* cells. Besides the cell elongation, the compound also disturbed the normal cell division. Treatment with actinomycin D resulted in filamentous *E. coli* cells, while single cells were observed in 1% DMSO treated *E. coli*. The results indicated that actinomycin D compounds had potential to be FtsZ inhibitor.

3.3.3 Effect of actinomycin D on GTPase activity of *Ec*FtsZ

In bacterial cell division, the mechanism of Z-ring formation is regulated by the polymerization and depolymerization of a FtsZ monomer. Since FtsZ is GTPase-like protein, the experiment was performed based on this knowledge. The addition of FtsZ inhibitor would result in inhibition of the GTPase activity of *Ec*FtsZ. Linear regression showed reduction in *Ec*FtsZ activity when the protein was treated with actinomycin D at various concentrations with IC_{50} of 20.06 µM (Figure 5). This reduction in phosphate amounts released in the reaction in different concentration of inhibitors, suggested that actinomycin D could inhibit *Ec*FtsZ function in a dose-dependent manner.

3.3.4 Effect of actinomycin D on FtsZ assembly

Actinomycin D disrupted the cytokinesis of *E. coli* JW0093 cells; therefore, the effects of the compound on the assembly of purified *E. coli* FtsZ were investigated *in vitro*. In this experiment, dynamic light scattering technique was adapted to determine *Ec*FtsZ polymerization by using Zetasizer Nano-ZS. The average size of *Ec*FtsZ particles with same diffusion coefficient of measured particles were measured as derived count rate (DCR) and calculated for evaluation as polymerization ratio. A decrease in the polymerization ratio value below 1.0 indicates a decrease in assembly of *Ec*FtsZ

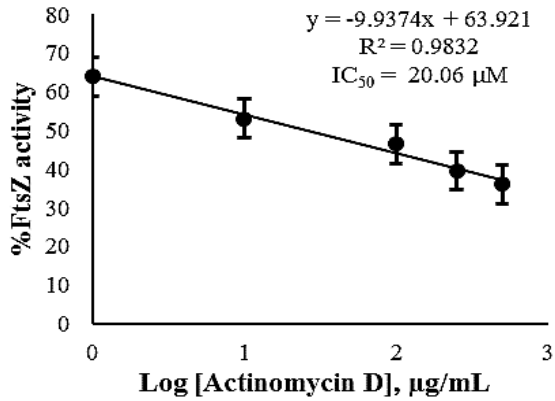

Figure 5. Effects of actinomycin D on GTPase activity of *Ec*FtsZ.

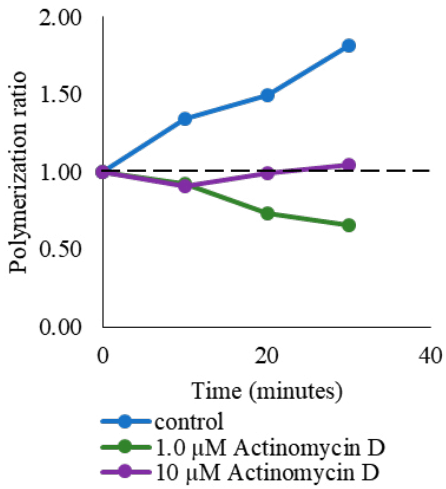

Figure 6. Effects of actinomycin D on the assembly of *Ec*FtsZ.

(Figure 6). As a consequence, the polymerization ratio was found to be decreased after adding 1, and 10 µM actinomycin D, polymerization ratio was close to 1.0 and lower indicating that polymerization of FtsZ protein did not occur. This suggested concentration-dependent inhibition of actinomycin D against *Ec*FtsZ assembly.

3.3.5 Prediction of binding interactions of actinomycin D at nucleotide binding site of *Ec*FtsZ

Total docking poses of actinomycin D obtained from flexible docking into the defined nucleotide binding pocket of *Ec*FtsZ were 30. The most possible binding pose was selected from the lowest CDOCKER_ENERGY and CDOCKER_INTERACTION_ENERGY scores. The best binding complex was selected with CDOCKER_ENERGY and DOCKER_INTERACTION_ENERGY of -34.7577 kcal/mol and -75.3212 kcal/mol), respectively.

Dynamic simulation of the best binding complex was performed for 10 ns. RMSD values of backbone atoms were calculated and plotted as

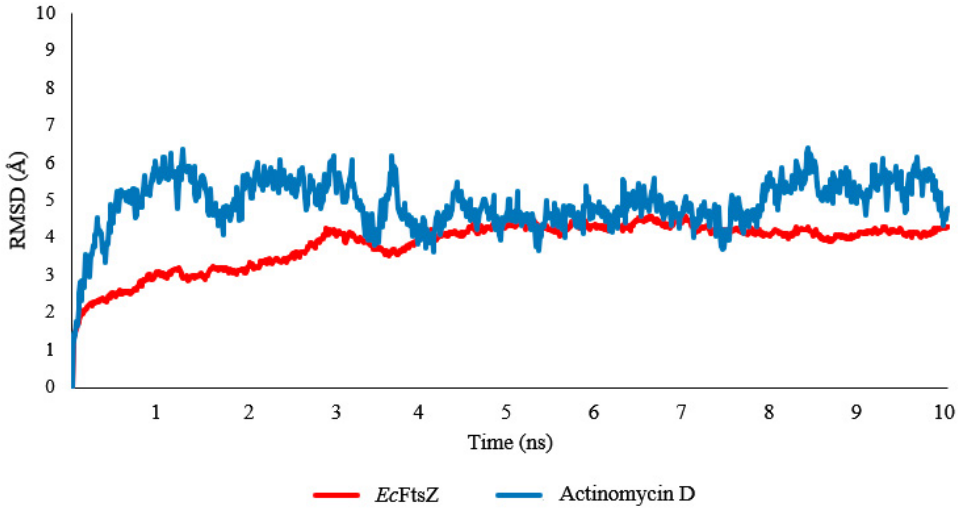

Figure 7. Time series of RMSD of *Ec*FtsZ protein (red line) and actinomycin D complex (red line).

Figure 8. Three-dimensional structure of actinomycin D bound to nucleotide binding site of *Ec*FtsZ.

in Figure 7. The complex stability was observed to archived equilibrium after 2 and 3 ns for FtsZ and actinomycin D, respectively.

The dynamically analysed binding complex of actinomycin D and *Ec*FtsZ at nucleotide binding site was shown in Figure 8 and was further analysed for the binding interaction in 2D diagram as shown in Figure 9 and interaction energies as reported in Table 2.

The result indicated that the GTP binding motif (106-GGAGTG-111) as well as Gly20 and Gly21 which was a part of T1 glycine-rich loop (19-GGGGG-23) [36] was found to interact with actinomycin D by van der Waals bond (Gly20, Asn24, Lys51, Gly67, Leu68, Ala70, Met104, Thr108, Lys133, Glu138, and Ans186), π-alkyl bond (Pro134, Phe135, Arg142, Leu178, Leu179, Phe182, and Ala185), and hydrogen bond (Gly21, Gly69, Gly103, Gly105, Thr132, Arg142, and Asn165).

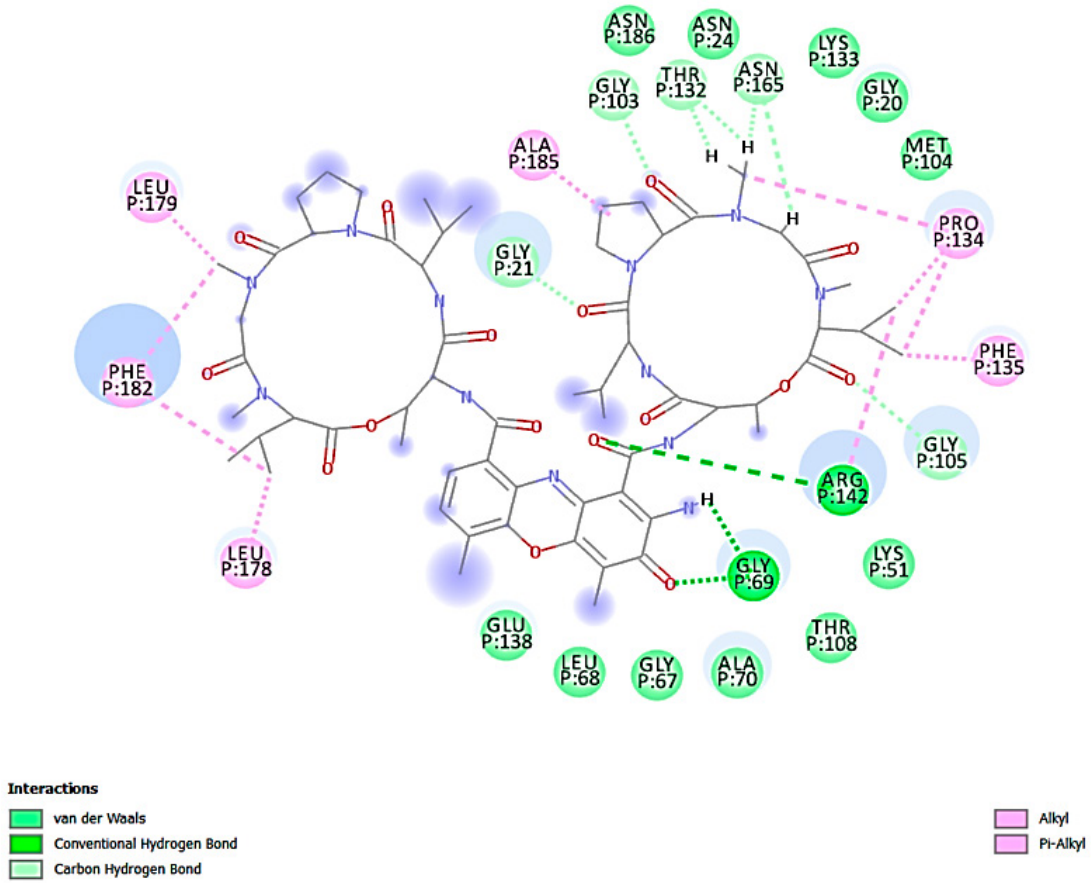

Figure 9. Two-dimensional interaction diagram of actinomycin D with van der Waals interacting residues (green circles) within a 4Å radius. Interactions of hydrogen bond with amino acid's side chain assigned by dashed line with different colors (bright green for conventional hydrogen bond and pale green for carbon hydrogen bond). The interaction by alkyl and π-alkyl bond were assigned in pink-colored circles and dashed lines.

The hydrogen bond formed with this residue was found to interact with phosphate side chain of GTP as previously described in other bacterial FtsZ-nucleotide complexes [37]. The conventional hydrogen bonds were formed from Gly69 and Arg142 residues to phenoxazine ring and amide linkage between phenoxazine ring and peptide ring, respectively. The interaction energies of both residues were -6.90311 and -11.09700 kcal/mol, respectively. Arg142 residue was found to have high binding affinity since this residue formed π-alkyl interaction with methyl group of methyl valine in the cyclic peptide of actinomycin D.

For π-alkyl interactions, Pro134 and Phe135 interacted with dimethyl group of methyl valine fragment of actinomycin D. Moreover, Pro134 also interacted with N-methyl of sarcosine part. While, Phe182 side chain which interacted with amino-purine ring of GTP was also involved in binding of actinomycin D in *Ec*FtsZ [30]. This compound was found to interact by π-alkyl bond with methyl group of methylvaline fragment (same

Table 2. Interaction energies per-residue within 4Å of actinomycin D in the nucleotide-binding pocket of *Ec*FtsZ.

Residue	Interaction Energy (kcal/mol)	VDW Interaction Energy (kcal/mol)	Electrostatic Interaction Energy (kcal/mol)
GLY20	-1.90761	-1.12457	-0.78304
GLY21	-8.17758	-3.29532	-4.88226
ASN24	-4.72232	-2.06929	-2.65303
LYS51	-14.38650	-0.15804	-14.22850
GLY67	-7.61184	-1.04044	-6.57140
LEU68	-1.70231	-1.14265	-0.55966
GLY69	-6.90311	-1.55727	-5.34584
ALA70	-2.45261	-3.56541	1.11280
GLY103	-6.52372	-1.52973	-4.99399
MET104	-3.79704	-1.84769	-1.94935
GLY105	-9.48717	-1.96066	-7.52651
THR108	-4.07824	-0.64933	-3.42891
THR132	-3.93805	-3.81205	-0.12600
LYS133	-0.98016	-0.88616	-0.09401
PRO134	-5.90087	-4.36054	-1.54033
PHE135	-3.74079	-2.37695	-1.36384
GLU138	-18.85340	-0.98970	-17.86370
ARG142	-11.09700	-6.05946	-5.03757
ASN165	-6.64832	-2.11420	-4.53412
LEU178	0.02086	-2.57977	2.60063
LEU179	1.44267	-2.73742	4.18009
PHE182	-9.03655	-9.26027	0.22372
ALA185	-2.80682	-1.44107	-1.36575
ASN186	-0.71802	-1.18015	0.46213

site of Leu178 binding interaction) and N-methyl group in sarcosine fragment (same site of Leu179 binding interaction) of the compound. Finally, Ala185 residue was found to interact with proline part of the compound by the same interaction. For the binding interaction energies of Pro134, Phe135, Phe182 and Ala 185 were -5.900870, -3.740790, -9.036550, and -2.806820 kcal/mol, respectively. The obviously low interaction energy of actinomycin D and Phe182 residue indicated a strong support for the binding to FtsZ protein as previously mentioned.

Lys51 residue was found to be a binding site of ZapA protein in order to promote FtsZ polymerization in prokaryotes [38, 39]. Actinomycin D interacted with this residue by strong interaction energies of -14.38650 kcal/mol. The change in Glu138 residue led to inhibition of Z-ring formation [40]. In our study, the complex also indicated strong binding between the compound

and this residue with interaction energies of -18.85340 kcal/mol.

The calculation of binding interaction energies of *Ec*FtsZ-actinomycin D complex showed that the total interaction energy was -134.00659 kcal/mol. This energy included the total van der Waals interaction energy and total electrostatic energy which were -57.73814 and -76.26845 kcal/mol, respectively. The strong interaction energies after dynamic simulation indicated the stability of the binding pose which also supported the potent result of GTPase inhibitory activity of actinomycin D as shown with its low IC_{50} value.

4. Conclusions

Actinomycin D isolated from *Streptomyces* sp. LT3-17 exhibited antibacterial and FtsZ inhibitory effects through the investigations on MIC and MBC assay against gram-positive and gram-negative bacteria, morphology analysis of FtsZ-overexpressed *E. coli* JW0093 and polymerization ratio of *Ec*FtsZ. The compound could elongate *E. coli* cells and inhibit FtsZ activity with potent IC_{50} value. In the study of polymerization of FtsZ, actinomycin D decreased the FtsZ polymerization with ratio less than 1.0. *In silico* study showed the binding behaviour and stability of *Ec*FtsZ-actinomycin D complex with interaction energies of binding residues. According to these results, actinomycin D contained potential to be FtsZ inhibitors. Thus, the information obtained from this study led to another discovery of novel antibacterial mechanism of actinomycin D as well as advantage for further development of novel FtsZ inhibitory agents.

Acknowledgments

The research was financially supported by Research Assistantships program of Faculty of Graduate Studies, Mahidol University. The authors would also like to thank the National BioResource Project Japan (NBRP)-*E. coli*/*B. subtilis* for providing the FtsZ-over expressed *E. coli* JW0093.

References

[1] World Health Organization. Antimicrobial resistance: global report on surveillance 2014; Available at: http://www.who.int/drugresistance/documents/surveillancereport/en/

[2] World Health Organization. The top 10 causes of death; Available at: https://www.who.int/news-room/fact-sheets/detail/the-top-10-causes-of-death

[3] Margolin W., *Nat. Rev. Mol. Cell Biol.*, 2005; **6**: 862-871. DOI 10.1038/nrm1745.

[4] Jan L., Fusinita E. and Amos L.A., *Annu. Rev. Biophys.*, 2004; **33**: 177-198. DOI 10.1146/annurev.biophys.33.110502.132647.

[5] Harold P.E., David E.A. and Masaki O., *Microbiol. Mol. Biol. Rev.*, 2010; **74**: 504-508. DOI 10.1128/MMBR.00021-10.

[6] Domadia P., Swarup S., Bhunia A., Sivaraman J. and Dasgupta D., *Biochem. Pharmacol.*, 2007; **74**: 831-840. DOI 10.1016/j.bcp.2007.06.029.

[7] Rai D., Singh J.K., Roy N. and Panda D., *Biochem. J.*, 2008; **410**: 147-155. DOI 10.1042/BJ20070891.

[8] Heine H.S., Purcell B.K., Bassett J., Miller L. and Goldstein B.P., *Antimicrob. Agents Chemother.*, 2010; **54(3)**: 991-996. DOI 10.1128/AAC.00820-09.

[9] Plaza A., Keffer J.L., Bifulco G., Lloyd J.R. and Bewley C.A., *J. Am. Chem. Soc.*, 2010; **132**: 9069-9077. DOI 10.1021/ja102 100h.

[10] Kanoh K., Adachi K., Matsuda S., Shizuri Y., Yasumoto K., Kusumi T., Okumura K. and Kirikae T., *J. Antibiot.*, 2008; **61**: 192-194. DOI 10.1038/ja.2008.29.

[11] Berdy J., *J. Antibiot.* 2005; **58(1)**: 1-26. DOI 10.1038/ja.2005.1.

[12] Bull A.T. and Stach J.E., *Trends Microbiol.*, 2007; **15**: 491-499. DOI 10.1016/j. tim.2007.10.004.

[13] Thawai C., Rungjindamai N., Klanbut K. and Tanasupawat S., *Int. J. Syst. Evol. Microbiol.*, 2017; **67**: 1451-1456. DOI 10.1099/ijsem.0.001736.

[14] Thawai C., Tanasupawat S., Itoh T., Suwanborirux K., Suzuki K. I. and Kudo T., *Int. J. Syst. Evol. Microbiol.*, 2005; **55**: 417-422. DOI 10.1099/ijs.0.63217-0.

[15] Thawai C., *Int. J. Syst. Evol. Microbiol.*, 2018; **68**: 1307-1312. DOI 10.1099/Ijse m.0.002672.

[16] Kelly K. L., *Inter-Society Color Council – National Bureau of Standard Color Name Charts Illustrated with Centroid Colors*., US Government Printing Office, Washington, DC, 1964.

[17] Tamaoka J., Determination of DNA Base Composition; in Goodfellow M. and O'Donnell A.G., eds., *Chemical Methods in Prokaryotic Systematics*, John Wiley and Sons, Chichester, 1994: 463-470.

[18] Weisburg W.G., Barns S.M., Pelletier D.A. and Lane D.J., *J. Bacteriol.*, 1991; **173**: 697-703. DOI 10.1128/jb.173.2.697-703.1991.

[19] Lane D.J., 16S/23S rRNA Sequencing; in Stackebrandt and Goodfellow M., eds., *Nucleic Acid Techniques in Bacterial Systematics*, Wiley and Sons, Chichester, 1991: 115-175.

[20] Yoon S.H., Ha S.M., Kwon S., Lim J., Kim Y., Seo H. and Chun J., *Int. J. Syst. Evol. Microbiol.*, 2017; **67**: 1616-1617. DOI 10.1099/ijsem.0.001755.

[21] Thompson J.D., Higgins D.G. and Gibson T.J., *Nucleic Acids Res.,* 1994; **22**: 4673-4680.

[22] Saitou N. and Nei M., *Mol. Biol. Evol.,* 1987; **4**: 406-425.

[23] Tamura K., Stecher G., Peterson D., Filipski A. and Kumar S., *Mol. Biol. Evol.,* 2013; **30**: 2725-2729. DOI 10.1093/molbev/m st 197.

[24] Felsenstein J., *Evolution*, 1985; **39**: 783-791. DOI 10.1111/j.1558-5646.1985.tb 00420.x.

[25] Ezaki T., Hashimoto Y. and Yabuuchi E., *Int. J. Syst. Bacteriol.,* 1989; **39**: 224-229. DOI 10.1099/00207713-39-3-224.

[26] Clinical and Laboratory Standards Institute (CLSI). *Methods for Dilution Antimicrobial Susceptibility Tests for Bacteria That Grow Aerobically*, Clinical and Laboratory Standards Institute, Wayne. 2012: 16-19.

[27] Charoenwiwattanakij P., Pratuangdejkul J., Jaturanpinyo M., Lowtangkitcharoen W., Suwanborirux K. and Nukoolkarn V., *Chiang Mai J. Sci.,* 2018; **45(7)**: 2566-2580.

[28] Tirado-Rives J. and Jorgensen W.L., *J. Med. Chem*., 2006; **49**: 5880-5884. DOI 10.1021 / jm060763i.

[29] Phillips J.C., Braun R., Wang W., Gumbart J., Tajkhorshid E., Villa E., Chipot C., Skeel R.D., Kale L. and Schulten K., *J. Comput. Chem.*, 2005; **26(16)**: 1781-802. DOI 10.1002/jcc.20289.

[30] Vanommeslaeghe K., Hatcher E., Acharya C., Kundu S., Zhong S., Shim J., Darian E., Guvench O., Lopes P., Vorobyov I., Mackerell Jr.A.D., *J. Comput. Chem.*, 2010; **31(4)**: 671-690. DOI 10.1002/jcc.21367.

[31] Feller S.E., Zhang Y., Pastor R.W. and Brooks B.R., *J. Chem. Phys.*, 1995; **103**: 4613-4621. DOI 10.1063/1.470648.

[32] Darden T., York D. and Pedersen L., *J. Chem. Phys.,* 1993; **98(12)**: 10089-10092. DOI 10.1063/1.464397.

[33] Wayne L.G., Brenner D.J., Colwell R.R., Grimont P.A.D., Kandler O., Krichevsky M.I., Moore L.H., Moore W.E.C., Murray R.G.E., Stackebrandt E., Starr M.P. and Truper H.G., *Int. J. Syst. Evol. Microbiol.*, 1987; **37**: 463-464. DOI 10.109 9/00207713-37-4-463.

[34] Byron H.A. and Karst H., *Biochemistry-US*, 1970; **9(20)**: 3976-3983. DOI 10.1021/bi00822a016.

[35] Chin Y. and Yu-yu T., *Eur. J. Biochem.,* 1992; **209**: 181-187. DOI 10.1111/j.1 432-1033.1992. tb17275.x.

[36] Diaz J.F., Kralicek A., Mingorance J., Palacios J.M., Vicente M. and Andreu J.M., *J. Biol. Chem.*, 2001; **276(20)**: 17307-17315. DOI 10.1074/jbc.M010 920200.

[37] Sheranaravenich K., Chongruchiroj S., and Pratuangdejkul J., *Pharm. Sci. Asia*, 2011; **38**: 19-31.

[38] Roseboom W., Nazir M.G., Meiresonne N.Y., Mohammadi T., Verheul J., Buncherd H., Bonvin A.M.J.J., Koning L.J.D., Koster C.G.D., Jong L.D. and Blaauwen T.D., *Int. J. Mol. Sci.* 2018; **19(10)**: 2928. DOI 10.3390/ ijms19102928.

[39] Gueiros-Filho F.J. and Losick R., *Gene Dev.*, 2002; **16**: 2544-2556. DOI 10.1101/ gad.1014102.

[40] Redick S.D., Stricker J., Briscoe G. and Erickson H.P., *J. Bacteriol.*, 2005; **187(8)**: 2727-2736. DOI 10.1128/JB.18 7.8.2727-2736.2005.